Environ. Sci. Technol. **2005**, *39,* 1299−1308

Axial Flow Cyclone for Segregation and Collection of Ultrafine Particles: Theoretical and Experimental Study

YU-DU HSU,[†] HUNG MIN CHEIN,*[,†] TZU MING CHEN,[†] AND CHUEN-JINN TSAI[‡]

Environmental Nanotechnology Research Laboratory, Center for Environmental, Safety and Health Technology, Industrial Technology Research Institute, Hsinchu, Taiwan, and Institute of Environmental Engineering, National Chiao Tung University, Hsin Chu, Taiwan

In this study, an axial flow cyclone was designed, fabricated, and evaluated at different conditions of air flow rates (Q_0) and low-pressure environments (P), especially for the segregation and collection of ultrafine particles. An evaporation/condensation type of aerosol generation system consisting of tube furnace and mixing chamber was employed to produce test aerosols. The test aerosol was then classified by a differential mobility analyzer (DMA) and number concentration was measured by a condensation nuclei counter (CNC) and an electrometer upstream and downstream of the cyclone, respectively. The s-shaped curve of the collection efficiency in submicron particle size range was obtained to be similar to the traditional cyclone found in the literatures when the particles were larger than 40 nm at $Q_0 = 1.07, 0.455$ L(STP)/min, and $P = 4.8-500$ Torr. The curve was found to be fitted very well by a semiempirical equation described in this paper. For particles smaller than 40 nm, however, the collection efficiency was unusually increased as the particle diameter was decreased due to the fact that the diffusion deposition becomes the dominant collection mechanism in the low-pressure conditions. A model composed of centrifugal force and diffusion deposition is presented and used to fit the experimental data. The cyclone was demonstrated to separate and collect ultrafine particles effectively in the tested vacuum conditions.

Introduction

Nanotechnology has the potential to profoundly change our economy, to improve our standard of living, and to bring the next industrial revolution (*1*). Nanopowder production is one of the key technologies. Particle separation and collection play a very important role in the production process. In addition, particle contamination affects the product yield of semiconductor and optoelectronic manufacturing also creates a clogging problem of the pumping line. The manufacturing processes involve many kinds of chemicals, generating particulate matter such as SiO_2 and toxic As particles. In Taiwan, most of the companies currently install local scrubbers for the treatment of gaseous pollutants. However, fine and ultrafine particles often pass through the control equipment and deposit on the inside surface of the pumping line, eventually resulting in obstruction of the vacuum pump and process operation. There are several other devices that have been developed to collect ultrafine particles. For example, Kulkarni et al. (*2*) modified an electrostatic precipitator by enhancing the charging efficiency of the nanoparticle. Tsai et al. (*3*) developed an axial flow cyclone to capture fine particles at low-pressure conditions.

A cyclone is a simple control device for particle collection. The traditional cyclone has cutoff aerodynamic diameter larger than 1 μm at atmospheric pressure. Theoretically, a cyclone is able to separate and collect ultrafine particles in vacuum conditions. However, to the best of our understanding, there is a lack of published experimental studies. Kuo and Tsai (*4*) have compared theoretical collection efficiency with experimental data for tangential-inlet cyclones. They report that there are no theoretical collection efficiency data that can fit the experimental data very well from the known literature. They also suggest that a fluid Reynolds number (Re_f) significantly affects particle collection efficiency and that Re_f is defined by

$$Re_f = \frac{\rho U_i (D - D_e)}{2\mu} \tag{1}$$

where ρ is the density of air, U_i is the inlet velocity, D is the diameter of the cyclone body, D_e is the diameter of the cyclone outlet, and μ is the dynamic viscosity of air. Kuo and Tsai (*4*) and Moore and McFarland (*5*, *6*) have compared experimental data from different literature and concluded that the logarithm of dimensionless cutoff aerodynamic diameter ($\ln \Psi_{50}$) is proportional to the logarithm of the Reynolds number ($\ln Re_f$). The mentioned dimensionless cutoff aerodynamic diameter (Ψ_{50}) is denoted as follows:

$$\Psi_{50} = \sqrt{C} D_{pa50}/D \tag{2}$$

where D_{pa50} is the cutoff aerodynamic diameter and C is the slip correction factor.

Liu and Rubow (*7*) have studied particle losses and collection efficiencies of a cascade axial flow cyclone at 30 L(STP)/min. The Ψ_{50} is presented as 12.2, 7.9, 3.6, 2.05, and 1.0 μm. Weiss et al. (*8*) have designed two axial flow cyclones for dust sampling in workplace. The Ψ_{50} is 4.8 and 3.0 μm at the flow conditions of 8 and 50 L(STP)/min, respectively. Vaughan (*9*) has invented several types of cyclones, and the cutoff aerodynamic diameters are between 1.6 and 6.5 μm when the flow rate is from 1.24 to 3.75 L(STP)/min. Maynard (*10*) has designed and studied cyclones based on the simplified assumptions of flow field and particle motion. The referred studies are limited to ambient conditions and for fine or coarse particle collection. Bai and Biswas (*11*) developed a deposition model for log-normally distributed aerosols onto cylindrical surfaces in cross-flow. The Bai−Biswas model considered diffusion, thermophoresis, and coagulation for submicron aerosol without inertial force effect. An axial flow cyclone has been developed in an earlier study (*3*) for the capture of fine particles, and an empirical model has been established. In this paper, the experiment and model are extended to account for both inertia and diffusion effects in the range of ultrafine particles.

* Corresponding author telephone: +886-3-5913853; fax: +886-3-5918753; e-mail address: hmchein@itri.org.tw.
[†] Industrial Technology Research Institute.
[‡] National Chiao Tung University.

10.1021/es0491735 CCC: $30.25
Published on Web 01/06/2005

Theoretical Model

In the previous study (*3*), the particle collection model has been derived for an axial flow cyclone considering the centrifugal force only. The governing equation for the steady state takes the following expression in cylindrical coordinate:

$$v_r\frac{\partial c}{\partial r}+\frac{v_\theta}{r}\frac{\partial c}{\partial \theta}+v_z\frac{\partial c}{\partial z}=\frac{D}{r}\frac{\partial}{\partial r}\left(r\frac{\partial c}{\partial r}\right) \tag{3}$$

The air flow is pseudo-steady-state with respect to axes moving with a mean velocity v_θ, and the concentration gradient in z direction ($\partial c/\partial z$) is independent of r axis. v_r is the particle radial velocity. To obtain unique particle concentration (c) and diffusion coefficient (D), we assume that particles are monodispersive and particle−particle interactions are neglected. Therefore

$$\left(\frac{P-Nw}{2\pi r_{\min}N}\right)\bar{v}_\theta\frac{\partial c}{\partial z}=\frac{D}{r}\frac{\partial}{\partial r}\left(r\frac{\partial c}{\partial r}\right)-\frac{\tau\bar{v}_\theta^{\,2}}{r}\frac{\partial c}{\partial r} \tag{4}$$

where P means pitch of vanes, $\tau = d_{pa}{}^2c/18\mu$ is the particle relaxation time, d_{pa} is the aerodynamic diameter of particle, μ is viscosity of air, and C is the slip correction factor. Tsai et al. (*3*) has derived the tangential gas velocity in the vane section ($\bar{v}_\theta$) as

$$v_\theta=\frac{2r_{\min}QN}{(r_{\max}{}^2-r_{\min}{}^2)(P-Nw)} \tag{5}$$

and the steady-state particle radial velocity ($\bar{v}_r$) as

$$\bar{v}_r=\frac{\tau\bar{v}_\theta^{\,2}}{r}=\frac{4\tau r_{\min}{}^2Q^2N^2}{r(r_{\max}{}^2-r_{\min}{}^2)(P-Nw)^2} \tag{6}$$

Particle Deposition Due to Centrifugal Force. If centrifugal force dominates the deposition mechanism (i.e., $D \ll \tau\bar{v}_\theta{}^2$), then eq 4 can be written as

$$\left(\frac{P-Nw}{2\pi r_{\min}N}\right)\frac{\partial c}{\partial z}=-\frac{\tau\bar{v}_\theta}{r}\frac{\partial c}{\partial r} \tag{7}$$

To integrate the above equation over r, the solution is given as

$$\left(\frac{P-Nw}{4\pi r_{\min}N}\right)\frac{\partial c}{\partial z}(r_{\max}{}^2-r_{\min}{}^2)=\tau\bar{v}_\theta c \tag{8}$$

which satisfies the boundary condition at $r = r_{\max}$ that $c = 0$. The average concentration of particle over the cross section of vane of cyclone is defined by

$$\bar{c}=\frac{1}{\pi(r_{\max}{}^2-r_{\min}{}^2)}\int_{r_{\min}}^{r_{\max}}c\cdot 2\pi r\,\mathrm{d}r \tag{9}$$

On integrating eq 8 for c over r using the definition of eq 9, we have

$$\left(\frac{P-Nw}{4\pi r_{\min}N}\right)\frac{\partial \bar{c}}{\partial z}(r_{\max}{}^2-r_{\min}{}^2)=2\tau\bar{v}_\theta\bar{c} \tag{10}$$

To further extend the collection model, we integrate the above equation with respect to z and get the overall penetration (P_{en}) expression as

$$P_{en}=\frac{\bar{c}_{out}}{\bar{c}_{in}}=\exp\left(-\frac{8\pi r_{\min}N}{P-Nw}\frac{\tau\bar{v}_\theta}{(r_{\max}{}^2-r_{\min}{}^2)}n\zeta P\right)=\exp\left(-8\pi n\zeta St\frac{NP/(P-Nw)}{1+r_{\max}/r_{\min}}\right) \tag{11}$$

where ζ is a fitting constant that gives the best agreement between the theoretical particle collection efficiencies and the experimental data. $n\zeta$ is the total number of turns of the particle in the cyclone. The assumption is on the basis of same velocities between vane section and body section in eq 11. $St = \tau\bar{v}_\theta/(r_{\max} - r_{\min})$ is the Stokes number. c_{in} and c_{out} are particle concentrations at inlet and outlet, respectively. Hence particle collection efficiency (η) can be expressed as

$$\eta=1-\frac{\bar{c}_{out}}{\bar{c}_{in}}=1-\exp\left(-\frac{8\pi r_{\min}N}{P-Nw}\frac{\tau\bar{v}_\theta}{(r_{\max}{}^2-r_{\min}{}^2)}n\zeta P\right)$$
$$=1-\exp\left(-4\pi r_{\min}n\zeta St\frac{NP/(P-Nw)}{(r_{\max}+r_{\min})/2}\right) \tag{12}$$

At the condition $4\pi r_{\min}n\zeta St\{(NP/(P-Nw))/(r_{\max}+r_{\min})/2\} \ll 1$, eq 12 is reduced to the following expression:

$$\eta=4\pi r_{\min}n\zeta St\frac{NP/(P-Nw)}{(r_{\max}+r_{\min})/2} \tag{13}$$

which is similar to the expression derived by Tsai et al. (*3*). Setting the particle collection efficiency (η) as 0.5 in eq 12, the cutoff diameter (d_{p50}) is written as

$$d_{pa50}=\sqrt{\frac{9\mu(r_{\max}{}^2-r_{\min}{}^2)^2(P-Nw)^2\ln 2}{8\pi n\zeta Qr_{\min}{}^2N^2PC}} \tag{14}$$

which is also similar to the expression derived by Tsai et al. (*3*). To substitute eq 14 into eq 12, the particle collection efficiency can be written as

$$\eta=\frac{\bar{c}_{in}-\bar{c}_{out}}{\bar{c}_{in}}=1-\exp\left(-\ln 2\frac{d_{pa}{}^2}{d_{pa50}{}^2}\right)=1-\exp\left(-0.693\frac{d_{pa}{}^2}{d_{pa50}{}^2}\right)=1-\exp\left(-\frac{d_{pa}{}^2}{d'^2_{pa50}}\right) \tag{15}$$

where $d'_{pa50} = d_{pa50}/\sqrt{\ln 2}$. d'_{pa50} is approaching to the expression (denoted as eq 9 in the original article) derived by Tsai et al. (*3*), while vane thickness is ignored (that is, $w \to 0$, and then $P - Nw/P \to 1$).

Particle Deposition Due to Diffusion. If diffusion effect dominates the deposition mechanism (i.e., $D \gg \tau\bar{v}_\theta{}^2$), then eq 4 can be written as

$$\frac{P-Nw}{2\pi r_{\min}N}\bar{v}_\theta\frac{\partial c}{\partial z}=\frac{D}{r}\frac{\partial}{\partial r}\left(r\frac{\partial c}{\partial r}\right)=D\frac{\partial^2 c}{\partial r^2}+\frac{D}{r}\frac{\partial c}{\partial r} \tag{16}$$

Several researchers have studied (*12*−*17*) or summarized (*18*) the model of particle deposition on the inside surface of circular tube by diffusion at steady state. Same as the above assumption of pseudo-steady flow, we integrate eq 16 with respect to the r axis. Therefore

$$\frac{P-Nw}{2\pi r_{\min}N}\bar{v}_\theta\frac{\partial c}{\partial z}\left(\frac{r^2}{4}+A\ln r+B\right)=Dc \tag{17}$$

where A and B are integration constants. Using the boundary conditions

$$c = 0 \text{ at } r = r_{max} \text{ and } r_{min} \quad (18)$$

eq 18 is solved and rearranged to give the equation

$$P_{en} = \frac{c}{c_{in}} = \exp\left(-\frac{8\pi r_{min} N}{\bar{v}_\theta (P - Nw)} \frac{Dz}{(r_{max}^2 - r^2) - \frac{(r_{max}^2 - r_{min}^2)}{\ln(r_{min}/r_{max})} \ln\frac{r}{r_{max}}}\right) \quad (19)$$

and

$$\frac{\partial c}{\partial z} = \left(\frac{D}{(r_{max}^2 - r^2) - \frac{(r_{max}^2 - r_{min}^2)}{\ln(r_{min}/r_{max})} \ln\frac{r}{r_{max}}} \frac{8\pi r_{min} N}{\bar{v}_\theta (P - Nw)}\right) c \quad (20)$$

Taking average of eq 20 over the cross section of vane of cyclone using the definition of eq 9, we have

$$\bar{c} = -\frac{\bar{v}_\theta (P - Nw)}{8\pi r_{min} N D}\left(\frac{(r_{max}^2 + r_{min}^2)}{2} + \frac{(r_{max}^2 - r_{min}^2)}{\ln(r_{min}^2/r_{max}^2)}\right)\frac{\partial \bar{c}}{\partial z} \quad (21)$$

and

$$\frac{\bar{c}}{\bar{c}_{in}} = \exp\left(-\frac{8\pi r_{min} N}{\bar{v}_\theta (P - Nw)} \frac{Dz}{\frac{(r_{max}^2 + r_{min}^2)}{2} - \frac{(r_{max}^2 - r_{min}^2)}{\ln(r_{max}^2/r_{min}^2)}}\right) \quad (22)$$

The overall penetration of cyclone is further expressed as

$$P_{en} = \frac{\bar{c}_{out}}{\bar{c}_{in}} = \exp\left(-\frac{1}{\frac{(r_{max}^2 + r_{min}^2)}{2(r_{max}^2 - r_{min}^2)} - \frac{1}{\ln(r_{max}^2/r_{min}^2)}} \frac{8\pi r_{min} N}{\bar{v}_\theta (P - Nw)} \frac{DL}{r_{max}^2 - r_{min}^2}\right) \quad (23)$$

where L is the effective length of cyclone. Equation 23 is similar to the governing equation of diffusion battery with annular tube and can be solved. The solution (only being taken a term of series) is written as

$$P_{en} = \frac{\bar{c}_{out}}{\bar{c}_{in}} = \exp\left(-\frac{8\pi r_{min} N}{\bar{v}_\theta (P - Nw)} \frac{1}{r_{max}^2 - r_{min}^2} DL\right) = \exp\left(-\frac{4\pi DL}{Q}\right) \quad (24)$$

To compare eq 23 to eq 24 in our study case (r_{max} = 1.5 cm and r_{min} = 1.0 cm), eq 23 can be simplified as

$$P_{en} = \frac{\bar{c}_{out}}{\bar{c}_{in}} = \exp\left(-\frac{8\pi r_{min} N}{\bar{v}_\theta (P - Nw)} \frac{15}{r_{max}^2 - r_{min}^2} DL\right) = \exp\left(-15 \times \frac{4\pi DL}{Q}\right) \quad (25)$$

where a factor of 15 is found in the numerator of the exponent term relative to annular tube.

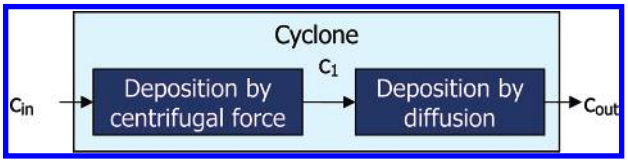

FIGURE 1. Particle collection of cyclone using the method of decomposing deposition effects due to centrifugal force and diffusion.

Particle Deposition Due to both Diffusion and Centrifugal Force. Obviously, there is a region where both diffusion and centrifugal force are important. The governing equation of eq 4 describes this region and is rewritten as

$$\left(\frac{P - Nw}{2\pi r_{min} N}\right)\bar{v}_\theta \frac{\partial c}{\partial z} = \frac{D}{r}\frac{\partial}{\partial r}\left(r\frac{\partial c}{\partial r}\right) - \frac{\tau \bar{v}_\theta^2}{r}\frac{\partial c}{\partial r} = \frac{D}{r}\frac{\partial}{\partial r}\left(r\frac{\partial c}{\partial r}\right) - Pe\frac{D}{r}\frac{\partial c}{\partial r} \quad (26)$$

where $Pe = \tau \bar{v}_\theta^2/D = (\tau \bar{v}_\theta^2/r_{min})r_{min}/D = \bar{v}_r r_{min}/D$ is the Peclet number. The Peclet number is a measure of domination mechanism between convection diffusion and molecular diffusion. To better fit the data and explain the collection mechanism, a modified model (that means no interaction between centrifugal force and diffusion effect) of the cyclone capturing ultrafine particles is derived. Figure 1 shows the idea of the modified model. The number concentration of airborne particle is decreased from c_{in} to c_{out} when the aerosol flow passes through the cyclone. The overall collection efficiency of cyclone is hence calculated by the following expression:

$$\eta = 1 - P_{en} = 1 - \frac{c_{out}}{c_{in}} \quad (27)$$

In a typical theory of cyclone, the mechanism of particle collection is the centrifugal force caused by the vortex of air flow. In the modified model shown as Figure 1, we assume that particle deposition is not only due to centrifugal force but also due to diffusion effect for ultrafine particles in vacuum conditions. Furthermore, the two mechanisms are acting independently and affecting particle collection in series. In another word, the interaction between centrifugal force and diffusion is ignored. Therefore eq 27 can be rewritten as follows:

$$\eta = 1 - P_{en}^{\text{diffusion}} P_{en}^{\text{centrifugal}} = 1 - \frac{c_{out}}{c_1}\frac{c_1}{c_{in}} \quad (28)$$

where $P_{en}^{\text{diffusion}}$ and $P_{en}^{\text{centrifugal}}$ are the penetration of particle due to diffusion and centrifugal force, respectively. c_1 is the number concentration in a virtual point of the cyclone. $P_{en}^{\text{centrifugal}}$ is directly obtained from eq 12 or eq 15 ($P_{en}^{\text{centrifugal}} = 1 - \eta^{\text{centrifugal}}$). On the other hand, $P_{en}^{\text{diffusion}}$ is calculated from eq 23. Gormley and Kennedy (*12*) have solved a steady-state equation of particle diffusion from a laminar pipe flow

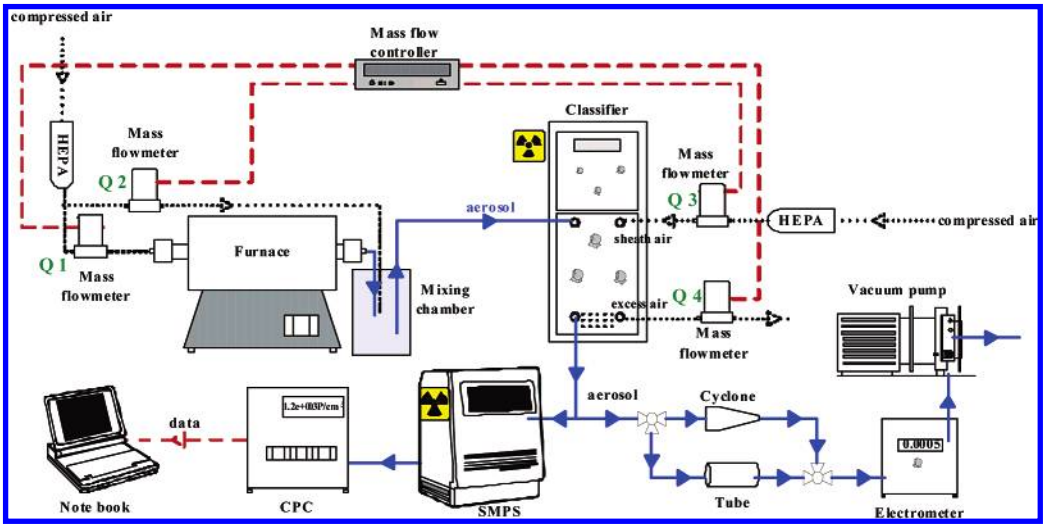

FIGURE 2. Schematic diagram of the cyclone efficiency test system.

and is expressed as an infinite dimensionless series (variables are rewritten by authors):

$$P_{en}^{\ diffusion} = \frac{c_{out}}{c_1} = 0.819\exp(-3.66\Pi) + 0.0975\exp(-22.3\Pi) + 0.0325\exp(-57\Pi) + \ldots$$

for $\Pi = \pi DL/Q > 0.02$

$$P_{en}^{\ diffusion} = \frac{c_{out}}{c_1} = 1 - 2.56\Pi^{2/3} + 1.2\Pi + 0.1767\Pi^{1/3} + \ldots$$

for $\Pi = \pi DL/Q < 0.02$ (29)

where Q is the volumetric air flow rate through the cyclone.

To integrate eq 26 with respect to the r axis, we have the following expression:

$$c = \left(\frac{P - Nw}{2\pi r_{min} N}\right)\frac{\bar{v}_\theta}{D}\frac{\partial c}{\partial z}\left(\frac{r^2}{2 - Pe} - \frac{E}{Pe} + Fr^{Pe}\right) \quad (30)$$

where E and F are integration constants. Using the boundary conditions $c = 0$ at $r = r_{max}$ and r_{min}, eq 30 can be solved and expressed as follows:

$$\frac{c}{c_{in}} = \exp\left(-\frac{2\pi r_{min} N}{P - Nw}\frac{2 - Pe}{r_{max}^{\ 2} - r_{min}^{\ 2}}\frac{Dz}{\bar{v}_\theta}\frac{1}{\dfrac{r_{max}^{\ 2} - r^2}{r_{max}^{\ 2} - r_{min}^{\ 2}} - \dfrac{r_{max}^{\ Pe} - r^{Pe}}{r_{max}^{\ Pe} - r_{min}^{\ Pe}}}\right) \quad (31)$$

and

$$c = -\left(\frac{P - Nw}{2\pi r_{min} N}\right)\frac{\bar{v}_\theta}{D}\frac{\partial c}{\partial z}\frac{r_{max}^{\ 2} - r_{min}^{\ 2}}{2 - Pe}\left(\frac{r_{max}^{\ 2} - r^2}{r_{max}^{\ 2} - r_{min}^{\ 2}} - \frac{r_{max}^{\ Pe} - r^{Pe}}{r_{max}^{\ Pe} - r_{min}^{\ Pe}}\right) \quad (32)$$

Using the definition of eq 9, the average concentration of particle over the cross section of vane of cyclone can be written as

$$\bar{c} = \frac{-1}{(r_{max}^{\ 2} - r_{min}^{\ 2})}\frac{P - Nw}{2\pi r_{min} N}\frac{\bar{v}_\theta}{D}\frac{\partial \bar{c}}{\partial z}\frac{r_{max}^{\ 2} - r_{min}^{\ 2}}{2 - Pe}\int_{r_{min}}^{r_{max}}\left(\frac{r_{max}^{\ 2} - r^2}{r_{max}^{\ 2} - r_{min}^{\ 2}} - \frac{r_{max}^{\ Pe} - r^{Pe}}{r_{max}^{\ Pe} - r_{min}^{\ Pe}}\right)dr^2$$

$$= \frac{-1}{2 - Pe}\frac{P - Nw}{2\pi r_{min} N}\frac{\bar{v}_\theta}{D}\frac{\partial \bar{c}}{\partial z}\left(\frac{(r_{max}^{\ 2} - r_{min}^{\ 2})}{2} - \frac{Pe(r_{max}^{\ 2} - r_{min}^{\ 2})r_{max}^{\ Pe} - 2r_{min}^{\ 2}(r_{max}^{\ Pe} - r_{min}^{\ Pe})}{(2 + Pe)(r_{max}^{\ Pe} - r_{min}^{\ Pe})}\right) \quad (33)$$

The solution is given as

$$P_{en} = \frac{\bar{c}_{out}}{\bar{c}_{in}} = \exp\left(-\frac{4\pi r_{min} N}{(P - Nw)\bar{v}_\theta}\frac{(2 - Pe)DL}{\left(\dfrac{r_{max}^{\ 2} - r_{min}^{\ 2}}{2} + \dfrac{2r_{min}^{\ 2}}{2 + Pe}\right) - \dfrac{Pe(r_{max}^{\ 2} - r_{min}^{\ 2})r_{max}^{\ Pe}}{(2 + Pe)(r_{max}^{\ Pe} - r_{min}^{\ Pe})}}\right)$$

$$= \exp\left(-\left(\frac{2 - Pe}{\left(r_{max}^{\ 2} - r_{min}^{\ 2} + \dfrac{4r_{min}^{\ 2}}{2 + Pe}\right) - \dfrac{2Pe(r_{max}^{\ 2} - r_{min}^{\ 2})}{(2 + Pe)(1 - r_{max}^{\ Pe}/r_{min}^{\ Pe})}}\right)\frac{4\pi DL}{Q}\right)$$

$$= 1 - \eta \quad (34)$$

where the boundary conditions $c = c_{in}$ at $z = 0$ has been introduced. Taking Pe approach to zero, where diffusion dominates the deposition mechanism, eq 34 can be reduced to eq 23. Here we use the relation

$$\lim_{Pe \to 0}\frac{Per_{max}^{\ Pe}}{(r_{max}^{\ Pe} - r_{min}^{\ Pe})} = \frac{2}{\ln(r_{max}^{\ 2}/r_{min}^{\ 2})} \quad (35)$$

In the opposite limit, eq 34 is closed to eq 11 while Pe is large enough. If we use the two limits (eqs 11 and 23) of penetration

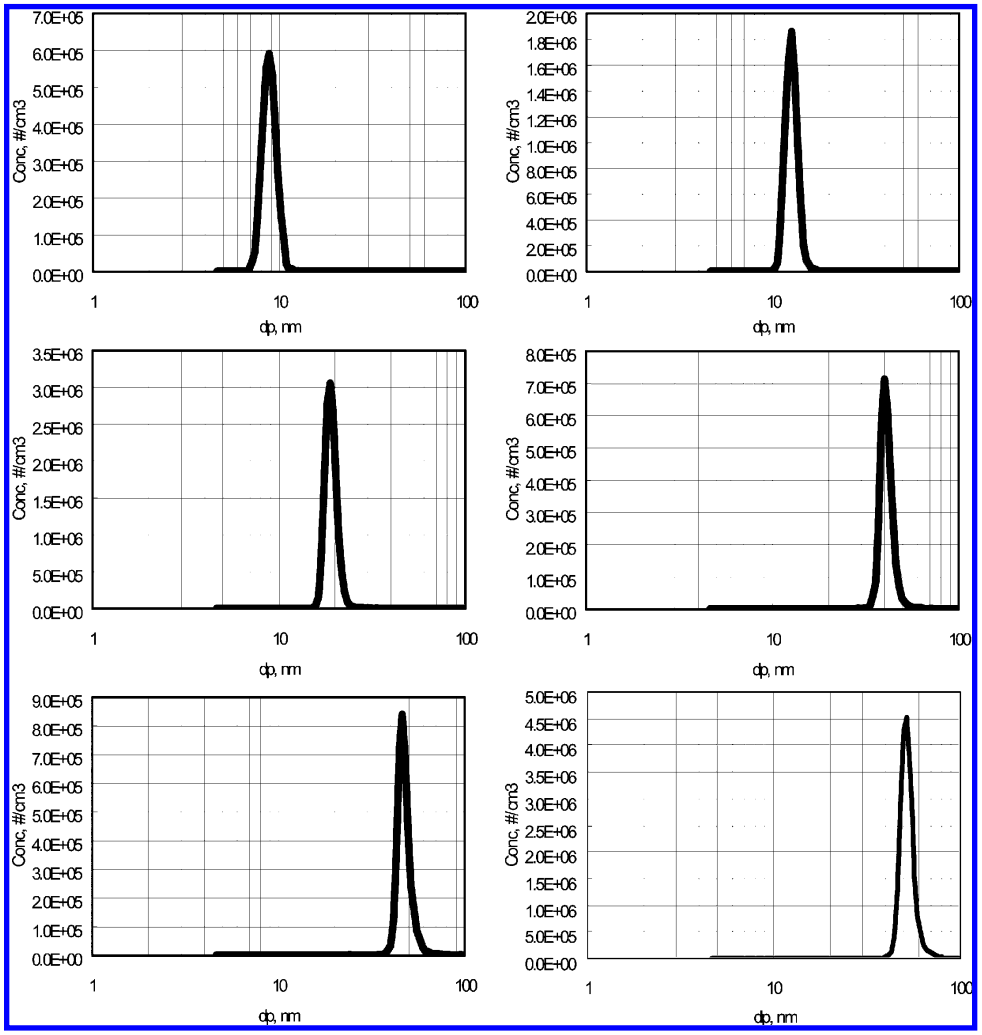

FIGURE 3. Typical size distributions of the generated test aerosol used to evaluate the cyclone collection efficiency.

to predict the curve in whole range, the ideal penetration of cyclone can be calculated as

$$\begin{aligned} P_{en} &= P_{en}^{\text{diffusion}} P_{en}^{\text{centfigual}} \\ &= \exp\left(-\left(\frac{1}{\frac{(r_{max}^2 + r_{min}^2)}{2(r_{max}^2 - r_{min}^2)} - \frac{1}{\ln(r_{max}^2/r_{min}^2)}} + Pe\right)\frac{4\pi DL}{Q}\right) \\ &= \exp\left(-\left(\frac{d_{pa50,diffusion}}{d_{pa}} + \frac{d_{pa}^2}{d_{pa50}^2}\right)\right) \\ &= 1 - \eta \end{aligned} \tag{36}$$

where d_{pa50} (see eq 14) is the centrifugal cutoff aerodynamic diameter in the range of deposition region due to centrifugal force. $d_{pa50,diffusion}$ as expressed in the following

$$d_{pa50,diffusion} = \frac{4n\zeta kTC}{3Q\mu \ln 2} \tag{37}$$

is the diffusive cutoff aerodynamic diameter in the range of diffusion deposition region.

Experimental Section

For the measurement of the cyclone collection efficiency, a test system was constructed as shown in Figure 2. The system includes three parts: aerosol generation, aerosol classifying and monitoring, and efficiency measurement of control device (cyclone). The aerosol generator, used in this study, is an evaporation/condensation system. In the configuration, filtered compressed air passes through a ceramic tube heated externally by a horizontal tube furnace. A ceramic boat containing oleic acid is located inside the tube. At the operating temperature of 190 °C, oleic acid (boiling point is 360 °C) exits as vapor due to its vapor pressure. The vapor of oleic acid provides a source of aerosol. The carrier gas with the aerosol source is then introduced into a mixing and dilution chamber to form liquid droplets of oleic acid by condensation mechanism. The polydisperse aerosol obtained from the generation system passes through an electrostatic classifier (TSI Inc., model 3071) to generate the desired monodisperse aerosol. A scanning mobility particle sizer (SMPS, TSI Inc.) is employed to measure and monitor the aerosol size distribution and number concentration. The aerosol flow passes an orifice (O'Keefe Controls Co., V-9) limiting the flow rate at 0.455 L(STP)/min and enters the test system composed of a tube and a cyclone in parallel. An electrometer (TSI model 3068) is used to measure the currents carried by the test aerosols downstream of the tube or cyclone. The measured collection efficiency (η) of the cyclone is calculated from the following equation:

$$\eta = 1 - \frac{I_{cyclone}(d_p)}{I_{tube}(d_p)} \tag{38}$$

where $I_{cyclone}$ and I_{tube} are the currents as the aerosol flow passes through the cyclone and the tube, respectively. A vacuum pump (0B32-1010m, Alcatel Vacuum Technology,

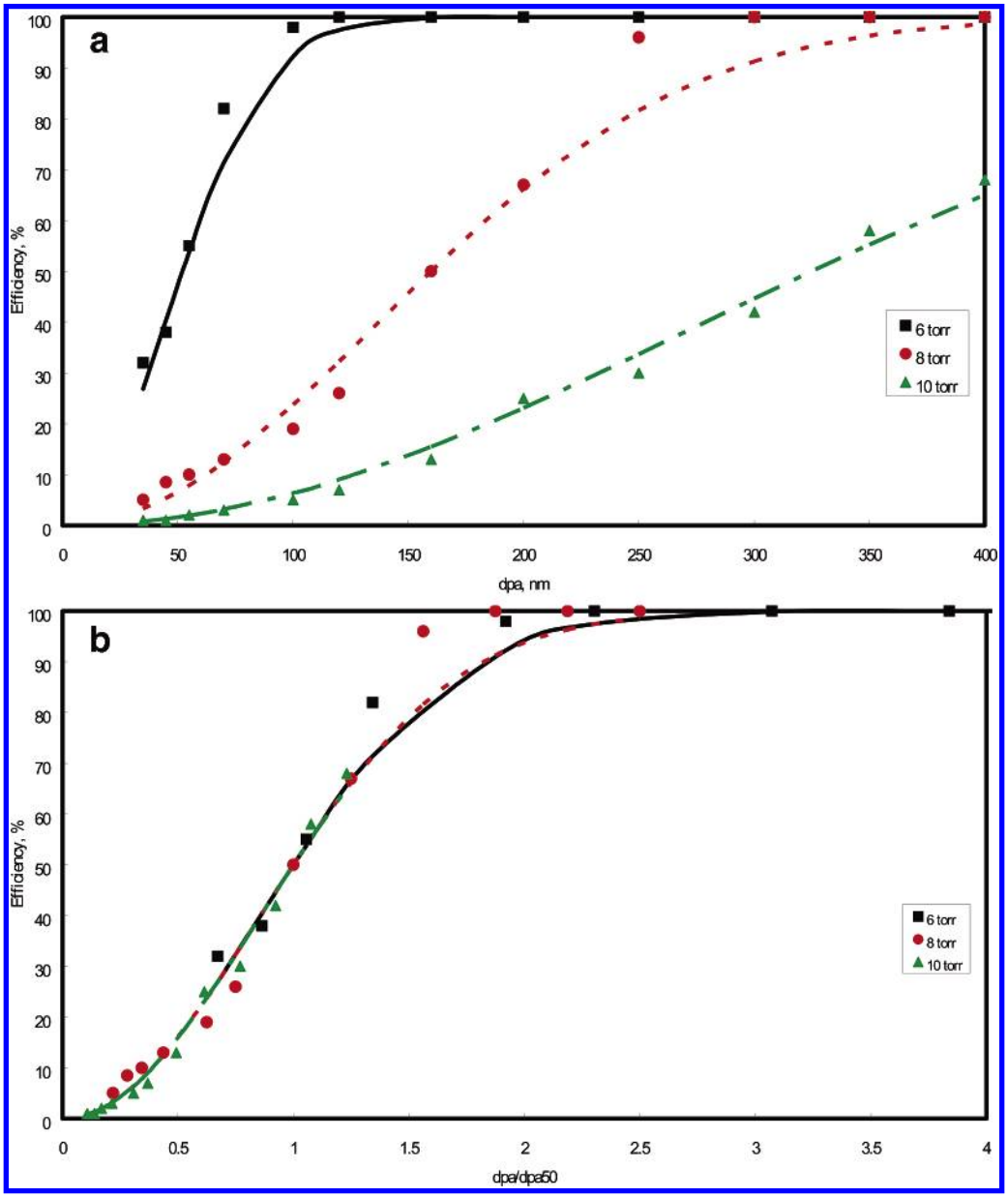

FIGURE 4. Experimental data and theoretical collection efficiency curve of the designed cyclone for particles lager than 40 nm at 0.455 L(STP)/min: (a) efficiency vs d_{pa}; (b) efficiency vs d_{pa}/d_{pa50}.

France; nominal pumping capacity, 600 L/min) and pressure gauges (MKS Baratron type, 626A13TAE, 1000 Torr max; and MKS Baratron type, 626A11TAE, 10 Torr max) were connected to keep the low pressure and to monitor the pressure in the test system, respectively.

Results and Discussion

The information of the test aerosol larger than 50 nm was shown in the previous study (*3*). The size distribution and number concentration of the generated nanoparticles are shown in Figure 3. Table 1 summarizes the characteristics of the nanoparticles used to evaluate the cyclone collection efficiency. The NMD ranges from 8.8 to 51.6 nm, and the GSD ranges from 1.08 to 1.10, respectively. The total number concentration increases from about 5.6×10^4 to 3.7×10^5 no./cm^3 as the particle diameter increases from 8.8 to 51.6 nm.

Figures 4 and 5 compare the experimental data of particle collection efficiencies with the calculated results using eq 15 at various pressures and flow rates. r_{max} and r_{min}, the inner radius of the cyclone and the radius of the vane spindle, are 1.5 and 1.0 cm, respectively. The s-shaped curves of cyclone collection efficiency are observed for particle larger than about 40 nm. The calculation results from the previous study (*3*) are used for d_{pa50}. The present model (eq 15) fits very well with the experimental data as shown in Figures 4a and 5a. Especially, the present model can generally fit the experimental data with the same curve in varying pressure conditions, as shown in Figures 4b and 5b. The curve has been displayed in the way as the collection efficiency (η) is a function of d_{pa}/d_{pa50}, which is the general curve for different test conditions considering centrifugal force only. In fact, Figures 4b and 5b can be combined as the same collection efficiency curve as explained in eq 15. It is the same as the previous study (*3*), a fitting constant ζ is introduced to match the theoretical model (eq 14) with experimental data.

Figures 6 and 7 show the trends of derived models considering centrifugal force and diffusion deposition. As particle diameter (d_p) increased and then the dimensionless parameter *Pe* (Pelect number) approaches infinite, the centrifugal force dominates. In the opposite limit, that is *Pe* close to zero, the diffusion effect dominates. In the two limits,

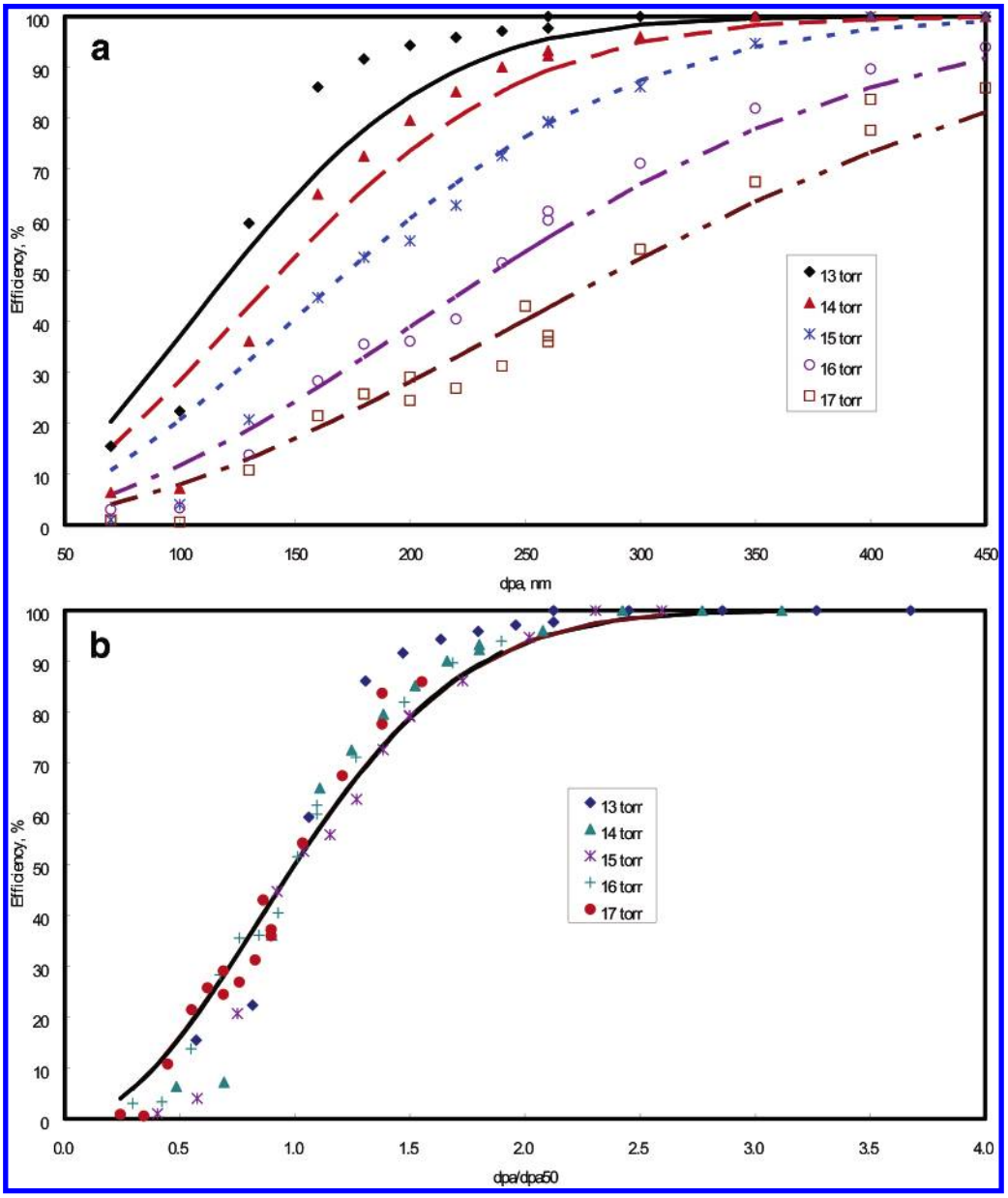

FIGURE 5. Experimental data and theoretical collection efficiency curve of the designed cyclone for particles larger than 60 nm at 1.07 L(STP)/min: (a) efficiency vs d_{pa}. (b) efficiency vs d_{pa}/d_{pa50}.

the collection efficiencies are up to 100%. Both inertia and diffusion mechanisms are considered when *Pe* is close to unity. In this case, the minimum collection efficiency is observed from the model and experiment.

Figure 6a shows the curve of the modified theoretical model considering both centrifugal force and diffusion deposition as described in eqs 34 and 36) at varying pressure and a fixed flow rate of 1.07 L(STP)/min. The model shows that there are different curves of cyclone collection efficiency at various pressures in the region of centrifugal force domination. However, the above-mentioned curves are close to an identical curve when the particle diameter decreases so that the dominated effect is changed to diffusion deposition. Figure 6b shows the curve of the modified theoretical model considering both centrifugal force and diffusion deposition at varying flow rate and a fixed pressure of 5 Torr. Similar results as shown in Figure 6a were observed in the curves of Figure 6b. In the transition region, the efficiency calculated by the simplified model (eq 36) is higher than that

TABLE 1. Summary of the Characteristics of the Nanoparticles Used To Evaluate the Cyclone Collection Efficiency[a]

item	NMD[b]	GSD[c]	total concn (no./cm^3)
1	8.8	1.09	55 911
2	9.8	1.10	24 799
3	10.6	1.08	74 203
4	12.1	1.08	88 133
5	12.6	1.08	146 908
6	12.9	1.08	334 430
7	18.9	1.08	230 664
8	28.2	1.09	137 851
9	40.6	1.09	52 322
10	47.6	1.10	319 771
11	46.6	1.09	60 275
12	51.6	1.10	368 814

[a] The system pressure is at 1 atm at the inlets of cyclone and reference tube (see Figure 2). The flow rates of carry air in furnace, inlet, and outlet of classifier (TSI 3071) are all kept at 1.3 or 0.755 L(STP)/min (depending on the requirement of cyclone test). The flow rate of SMPS (TSI 3080/3081) is 0.3 L(STP)/min. The flow rate of cyclone or reference tube is kept at 1.0 or 0.455 L(STP)/min by orifice. [b] NMD = number median diameter. [c] GSD = geometric standard deviation.

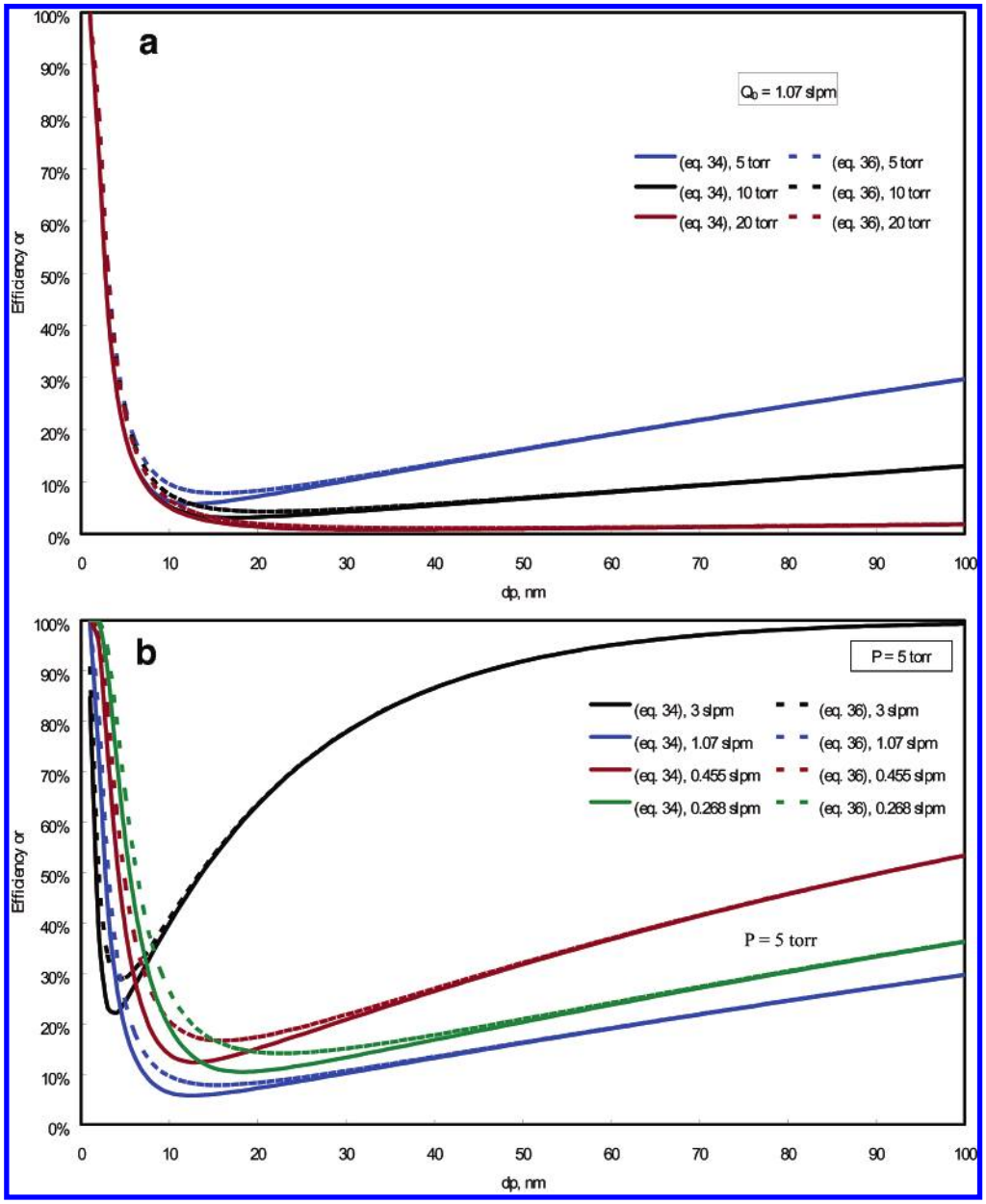

FIGURE 6. Theoretical model considering both centrifugal force and diffusion deposition at varying pressure (a) and at varying flow rate (b).

calculated by the theoretical model (eq 34). The maximum deviation is about 12%.

As compared with the same dimension of annular tube and based on the designed dimensions, $r_{max} = 1.5$ cm and $r_{min} = 1.0$ cm, of our axial flow cyclone, a factor of 15+ *Pe* is found in numerator of exponent term of eq 36 relative to eq 24, a penetration of a straight annular tube with plug flow. To recall eq 26, three main mechanisms dominate behavior of particles, that is axial convection, radial convection, and diffusion. Axial and radial transportation competition between the left and right sides of eq 26 is the key factor determining the capture efficiency of particles. The criterion for the largest efficiency is the maximum value of both radial terms on the right side of eq 26 as compared with the axial convection term on the left side. Alternatively, it might be expressed as the characteristic times including radial diffusion time $(r_{max}^2 - r_{min}^2)/D$, radial convection time $(r_{max} - r_{min})/\bar{v}_r = (r_{max} - r_{min})/(t\bar{v}_\theta^2/r_{min})$, and axial convection time $L/\bar{v}_z = L/(\bar{v}_\theta(P - Nw)/2\pi r_{min}N)$. Here L is the length of the cyclone. Therefore, the criterion to ignore radial convection may be written as

$$Pe \ll \frac{Q}{4\pi DL} \text{ or } St \ll \frac{r_{min}}{L} \tag{39}$$

To ignore radial diffusion, the criterion may be expressed as

$$\frac{Pe}{L} \gg \frac{St}{r_{max} + r_{min}} \tag{40}$$

or

$$Pe \gg St \tag{41}$$

when L is approximately equal to r_{max} or r_{min}.

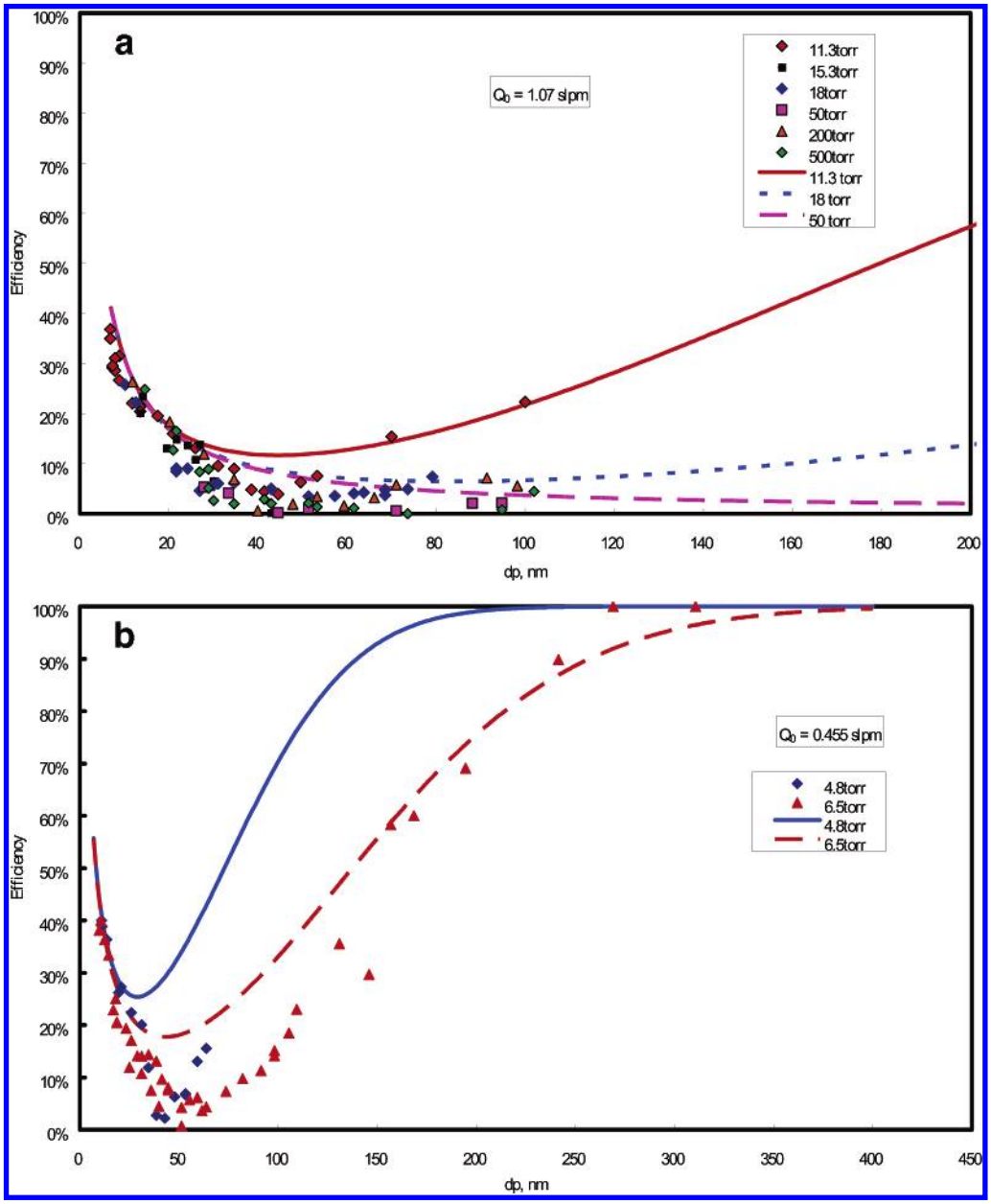

FIGURE 7. Comparing the experimental data with the theoretical model for different pressures at the same flow rate (a) 1.07 L(STP)/min, (b) 0.455 L(STP)/min. $P = 5$ Torr.

Another limit is the radial flow in a stationary medium. In the case

$$Pe \gg \frac{Q}{4\pi DL} \text{ or } St \gg \frac{r_{\min}}{L} \tag{42}$$

This means that the relative changes in radial concentration are large because the particles rapidly deposit on the wall; that is, the radial concentration gradient is high. In the other case, the radial diffusion time must be shorter compared with the axial convection time. The statement leads to the following condition:

$$\frac{Pe}{L} \ll \frac{St}{r_{\max} + r_{\min}} \tag{43}$$

If $St \gg r_{\min}/L$ and $St \gg (Pe/L)(r_{\max} + r_{\min})$ simultaneously exist, the capture efficiency of a cyclone can be kept at a high level regardless if the particle diameter is large or small. However, such a cyclone is sometimes difficult to design or unrealistic because of the economic reasons, the energy consumption is too high, or the tube is too long. The easier choice is to keep one of the above conditions only. The former is the design of a traditional cyclone; the latter is the design of a diffusion battery. In our designed axial flow cyclone, the range of low efficiency in the transition region is reduced while the pressure is decreased (Figure 7).

Figure 7a shows the experimental results of particle collection efficiency at 1.07 L(STP)/min. The range of particle diameter is from 6.85 to 100 nm. Figure 7b shows the experimental results of particle collection efficiency at 0.455 L(STP)/min. The range of particle diameter is from 9.82 to 313 nm. In the figure, the centrifugal cutoff aerodynamic diameters used in eq 36 are obtained by eq 14, and the diffusive cutoff aerodynamic diameters are calculated by eq 37. Here, the fitting constant ζ was assumed to be 1.5, which is suggested by Tsai et al. (*3*). As shown in Figure 7a, the measured collection efficiency is increased to 38% as the particle diameter is decreased to 6.85 nm due to the diffusion deposition in the nanoparticle size range. Figure 7b shows

similar results, which has a collection efficiency of 40% as particle diameter is equal to 9.82 nm. Vacuum pressures at the inlet (before the vane) and outlet (after the vane) of the cyclone were measured. At 1.07 L(STP)/min, the highest vacuum achieved is 11.3 Torr at the cyclone body, and the pressure drop (inlet pressure minus body pressure) is 3.5 Torr. The pressure drop decreases with an increasing cyclone-body pressure. At the body pressure of 500 Torr, the pressure drop becomes less than the lower limit of pressure gauge. Higher vacuum is achieved at lower volumetric flow rate. At 0.455 L(STP)/min, the highest vaccum achieved is 4.8 Torr at the cyclone outlet, and the pressure drop is 1.9 Torr. In this study, the outlet pressure was used to calculate particle collection efficiency from eqs 34 and 36.

On the basis of the modified model as shown in Figure 1 and described by eqs 28 and eq 36, the present experimental data were fitted with the model and shown in Figure 7. Here eqs 11 and 29 have been multiplied by the fitting constant ζ. Figure 7, panels a and b, shows the collection efficiencies splitting into different curves at the region where centrifugal force dominate the deposition mechanism. However, the collection efficiencies were approaching the same curve when the diffusion deposition dominates. This is due to the pressure effect on diffusion coefficient of the particle that increases the collection efficiency. The modified model expressed in eqs 28 and 36 has been demonstrated to effectively explain the particle deposition phenomena of the new cyclone, especially in the nanoparticle size range.

Literature Cited

(1) Roco, M. C. (NSET Chair), Supplement to the President's FY2004 Budget, National Nanotechnology Initiative, National Science and Technology Council, Committee on Technology, Subcommittee on National Science, Engineering, and Technology (NSET), 2003, p 1.

(2) Kulkarni, P.; Namiki, N.; Otani, Y.; Biswas, P. Charging of particles in unipolar coronas irradiated by in-situ soft X-rays: enhancement of capture efficiency of ultrafine particles. *J. Aerosol Sci.* **2002**, *33* (9), 1279−1296.

(3) Tsai, C.-J.; Chen, D.-R.; Chein, H. M.; Chen, S.-C.; Roth, J.-L.; Hsu, Y.-D.; Biswas, P.; Li, W. Theoretical and experimental study of an axial flow cyclone for fine particle removal in a vacuum conditions. *J. Aerosol Sci.* **2004**, *35* (9), 1105−1118.

(4) Kuo, K. Y.; Tsai, C. J. On the theory of particle cutoff diameter and collection efficiency of cyclones. *Aerosol Air Qual. Res.* **2001**, *1* (1), 47−56.

(5) Moore, M. E.; McFarland, A. R. Performance modeling of single-inlet aerosol sampling cyclones. *Environ. Sci. Technol.* **1993**, *27*, 1842−1848.

(6) Moore, M. E.; McFarland, A. R. Design methodology for multiple inlet cyclones. *Environ. Sci. Technol.* **1996**, *30*, 271−276.

(7) Liu, B. Y. H.; Rubow, K. L. A new axial flow cascade cyclone for size characterization of airborne particulate matter. In *Aerosols*; Liu, B. Y. H., Pui, D. Y., Fissan, H. J., Eds.; Elsevier: Amsterdam, 1984; pp 115−118.

(8) Weiss, Z.; Martinec, P.; Vitek, J. *Vlastnosti Dulnibo Prachu A Zaklady Protiprasne Techniky*; SNTL: Prague, 1987.

(9) Vaughan, N. P. Construction and testing of an axial flow cyclone pre-separator. *J. Aerosol Sci.* **1988**, *19* (3), 295−305.

(10) Maynard, A. D. A simple mode of axial flow cyclone performance under laminar flow conditions. *J. Aerosol Sci.* **2000**, *31* (2), 156−167.

(11) Bai, H.; Biswas, P. Deposition of lognormally distributed aerosols accounting for simultaneous diffusion, thermophoresis and coagulation. *J. Aerosol Sci.* **1990**, *21* (5), 629−640.

(12) Gormley, P. G.; Kennedy, M. Diffusion form a stream flowing through a cylindrical tube. *Proc. R. Irel. Acad.* **1949**, *A52*, 163−169.

(13) Sideman, S.; Luss, D.; Peck, R. E. Heat transfer laminar flow in circular and flat conduits with (constant) surface resistance. *Appl. Sci. Res.* **1965**, *A14*, 157−171.

(14) Davis, H. R.; Parkins, G. V. Mass transfer form small capillaries with wall resistance in the laminar flow regime. *Appl. Sci. Res.* **1970**, *22*, 20−30.

(15) Tan, C. W.; Hsu, C. J. Diffusion of aerosols in laminar flow in a cylindrical tube. *J. Aerosol Sci.* **1971**, *2*, 117−124.

(16) Lekhtmakher, S. O. Effect of Peclect number on the precipitation of partcles from a laminar flow. *J. Eng. Phys.* **1971**, *20*, 400−402.

(17) Bowen, B. D.; Levine, S.; Epstein, N. Fine particle deposition in laminar flow through parallelplate and cylindrical channels. *J. Colloid Interface Sci.* **1976**, *54*, 375−390.

(18) Baron, P. A., Willeke, K., Eds. *Aerosol Measurement*: *Principles, Techniques, and Applications*, 2nd ed.; John Wiley & Sons: New York, 2001.

Received for review June 3, 2004. Revised manuscript received August 30, 2004. Accepted September 15, 2004.

ES0491735